Quantitative analysis of hemocyte morphological abnormalities associated with Campoletis sonorensis parasitization

Authors: Turnbull, Matthew W., Martin, Stacy B., and Webb, Bruce A.

Source: Journal of Insect Science, 4(11) : 1-15

Published By: Entomological Society of America

URL: https://doi.org/10.1673/031.004.1101

Turnbull MW, Martin SB, Webb BA. 2004. Quantitative analysis of hemocyte morphological abnormalities associated with *Campoletis sonorensis* parasitization. 15pp. *Journal of Insect Science*, 4:11, Available online: insectscience.org/4.11

Journal of Insect Science

insectscience.org

Quantitative analysis of hemocyte morphological abnormalities associated with *Campoletis sonorensis* parasitization

Matthew W. Turnbull[1], Stacy B. Martin[2] and Bruce A. Webb[2]

[1]*Department of Entomology, Soils, and Plant Sciences, 114 Long Hall, Box 340315 Clemson University, Clemson, SC, U.S.A. 29634-0315.*

[2]*Department of Entomology, S-225 Agricultural Science Center, North, University of Kentucky, Lexington, KY U.S.A. 40546-0091*

turnbul@clemson.edu

Received 21 November 2003, Accepted 10 March 2004, Published 15 April 2004

Abstract

Endoparasitoids of arthropods evoke host cellular immune responses that result in hemocytic encapsulation of the endoparasitoid, unless these responses are disrupted by the parasite. Our interest has focused on mutualistic viruses found in some hymenopteran endoparasitoids that disrupt hemocyte function and prevent encapsulation. Specifically, the *Campoletis sonorensis* polydnavirus interacts with wasp factors to suppress immunity via expression of intracellular and secreted viral proteins. To study the roles of specific parasitization-associated factors on immunocyte morphology, fluorescence microscopy was used to visualize the actin cytoskeleton in infected and uninfected cells, or after treatment with *C. sonorensis* ovarian proteins or plasma from infected larvae. The titer and distribution of F- and G-actin were altered in hemocytes from parasitized insects relative to control cells, with plasma from parasitized larvae having an intermediate effect. This suggests that intracellular and secreted factors contribute to suppression of cellular immune responses in *C. sonorensis*.

Keywords: insect immunity, actin cytoskeleton, ovarian proteins, polydnavirus

Abbreviation:

*Cs*IV	*Campoletis sonorensis* ichnovirus
*Cs*OPs	*Campoletis sonorensis* ovarian proteins
FITC	fluorescein isothiocyanate

Introduction

Parasitoids must avoid host immune responses to survive. Endoparasitoids, in particular, are exposed to the host immune system as they develop in the hemocoel. In lepidopteran larvae the primary immune response is hemocytic encapsulation of multicellular parasites (Schmidt *et al.* 2001). In the lepidopteran *Pseudoplusia includens*, encapsulation involves two populations of hemocytes, granulocytes and plasmatocytes (Clark *et al.* 1997; Clark *et al.* 1998; Pech and Strand 1996; Strand and Clark 1999). Granulocytes recognize and opsonize a foreign object, by adhering, degranulating or both, and recruit plasmatocytes via release of the cytokine PSP-1. Plasmatocytes, normally unadherent and unable to spread in the hemocoel, are activated by PSP-1 and recruited to the site of immune response and adhere in multiple layers that flatten across the invader and ultimately surround it. The final step of encapsulation is the completion of the capsule by a single layer of granulocytes. Parasite death occurs through asphyxiation, starvation, or potentially through the release of cytotoxic chemicals (Schmidt *et al.* 2001).

Parasitoids have evolved passive strategies such as crypsis and molecular camoflauge to evade host immune surveillance as well as active strategies to overcome these defenses (Schmidt *et al.* 2001). Active strategies typically entail synthesis and release of proteins into the host hemocoel. Such molecules may be synthesized by the parasitoid (e.g. venoms), the egg membrane (e.g. teratocytes), the developing parasitoid, or by an associated virus that is introduced by the parasitoid during oviposition and which infects host cells. An example of the latter are the polydnaviruses, mutualistic viruses associated with certain hymenopterans. There are two groups of polydnaviruses, the ichnoviruses and bracoviruses, associated with the Ichneumonidae and Braconidae wasp families, respectively. Ichnoviruses and bracoviruses appear unrelated evolutionarily, but are thought to have convergently evolved under similar selection pressures (Turnbull and Webb 2002). Both ichnoviruses and bracoviruses have segmented DNA genomes encapsidated within virions but reside in the wasp genome as integrated proviral DNA, allowing for efficient vertical transmission. Viral DNA excision, replication and packaging into virions is limited to late pupal and

adult ovaries in both virus groups (Albrecht *et al.* 1994; Volkoff *et al.* 1995). Virus is delivered to the hemocoel of lepidopteran hosts during parasitization, along with the wasp egg, ovarian proteins, and venom. Hemocytes are efficiently infected by polydnaviruses although other tissues are also infected. Virus replication is not observed in parasitized hosts (Strand *et al.* 1992; Theilmann and Summers 1986) although transcription of viral genes occurs in infected cells. Virus infection and expression of polydnavirus-encoded proteins is required for successful parasitization and induces pathologies such as altered host development (Cusson *et al.* 2000; Pennacchio *et al.* 1998; Soller and Lanzrein 1996), reduced humoral immunity (Shelby *et al.* 2000), and abrogation of cellular immunity (Cui *et al.* 2000; Strand 1994).

In the ichneumonid wasp *Campoletis sonorensis,* ovarian proteins (*Cs*OPs) that are injected with the associated ichnovirus (*Cs*IV) and the wasp's egg during parasitization reduce encapsulation prior to transcription of viral genes. Hemocytes treated with *Cs*OPs exhibit morphological and microfilament abnormalities (Luckhart and Webb 1996; Webb and Luckhart 1994). As virus infection and expression progress, the effects of *Cs*IV-encoded proteins supercede the transient effects of *Cs*OPs (Luckhart and Webb 1996; Webb and Luckhart 1996). The viral genes belonging to the cys-motif gene family are most abundantly expressed (Blissard *et al.* 1986; Cui and Webb 1996; Dib-Hajj *et al.* 1993). The *Cs*IV cys-motif proteins VHv1.1 and VHv1.4 are secreted from infected cells and bind to hemocytes where they are endocytosed (Cui *et al.* 1997; Li and Webb 1994). Recombinant VHv1.1 protein qualitatively reduces encapsulation and induces abnormalities in the F-actin cytoskeleton (Li and Webb 1994). There are 10 cys-motif genes encoded by *Cs*IV and all are transcribed in infected lepidopterans. All 10 cys-motif genes encode signal peptides, and are the only genes encoded by *Cs*IV having predicted signal peptides (Webb *et al.*, in prep.). Treatment of normal hemocytes with cell-free plasma isolated from parasitized insects alters responses of these cells to immune stimuli *in vitro* (Turnbull *et al.*, personal observations), suggesting that some hemocyte immune pathologies are due to the cys-motif proteins. Given the large number of secreted cys-motif proteins it is tempting to speculate that secreted factors alone cause immune suppression, but studying the effects of these proteins individually and in combination requires the ability to precisely measure and quantify the effects of viral proteins on hemocyte morphology and function.

Actin cytoskeleton staining of hemocytes from parasitized lepidopterans with FITC-phalloidin (Schmidt *et al.* 2001; Stettler *et al.* 1998; Strand and Pech 1995) has been used to enhance visualization of cell morphology. This has demonstrated that the F-actin cytoskeleton appears to be disrupted by many parasitoids, which probably evolved as a means to disrupt hemocytic immunity. To further delineate factors and targets responsible for immune suppression and inhibition of hemocytic encapsulation in parasitized larvae, we have developed semi-quantitative fluorescent microscopy assays. These assays provide superior visualization of hemocyte morphology and better assessment of actin titer and distribution. In this report we show that infected cells fail to form cytoplasmic processes (i.e. they fail to spread) and have reduced titer and abnormal distribution of both G- and F-actin relative to control hemocytes. Treatment of control cells with plasma from parasitized larvae alters cell morphology although less so than virus infection. Thus, infection also induces some of the pathologies observed in parasitized hemocytes, in addition to the effects of secreted proteins.

Materials and Methods

Insect maintenance and parasitization

Maintenance of *Campoletis sonorensis* (Hymenoptera: Ichneumonidae) and *Heliothis virescens* (Lepidoptera: Noctuidae), a permissive host, were as previously described (Krell *et al.* 1982). Female *C. sonorensis* were added to *H. virescens* at a 1:3 ratio and allowed to parasitize *en masse* for at least 4 hours. In most cases, caterpillars were dissected to ensure that they had been parasitized. For all experiments, *H. virescens* were staged to attempt to minimize endocrinological and developmental effects on hemocyte types (Gardiner and Strand 2000) and hemolymph chemistry.

Hemocyte isolation and spreading

For time course and plasma overlay experiments, a caterpillar was bled from an abdominal proleg pierced with a glass needle into 100 µl PBS (0.1 M NaCl, 9.6 mM Na_2HPO_4, 15.4 mM NaH_2PO_4, pH 6.8) on a coverslip in a humid chamber. For ovarian protein overlays, 20 control 3rd instar *H. virescens* were bled into 2 ml cold PBS on ice. Cells were resuspended by gentle pipetting and 100 µl aliquots of the hemolymph suspension were applied to coverslips. After 7 min, unattached cells and any remaining hemolymph were removed and the cells were washed with several volumes of PBS to inhibit melanization. One hundred microliters of PBS or an experimental treatment was overlaid on the cells and the cells were allowed to spread for 1 hour at 25° C.

Treatment preparations

Pooled plasma was obtained by bleeding parasitized larvae from abdominal prolegs into 100 µl ice cold PBS. Hemocytes were removed from the suspension by centrifugation at 800 x g for 5 min at 4° C and a sample of plasma checked by light microscopy to ensure removal of cells.

Campoletis sonorensis ovarian proteins (*Cs*OPs) were isolated as previously described (Webb and Luckhart 1994). Ovaries from 200 adult female *C. sonorensis* were dissected in PBS, minced and transferred to 200 µl cold PBS for homogenization. The mixture was centrifuged for 5 seconds at maximum speed, and the supernatant transferred to the top of a 30% (w/v) sucrose/PBS gradient, while 200 µl cold PBS was transferred to another gradient as a negative control. The tubes were centrifuged at 50,000 x g for 1 hour at 5° C. The top 750 µl fraction of each tube was purified and the 29-36 kDa *Cs*OP complex (Webb and Luckhart 1994) concentrated by 4X PBS washes on a 10 kDa filter (Micron) to a final volume of 200 µl, which was aliquoted and stored at –80° C until use. The purity of the preparation was ascertained by Coomassie-stained SDS-PAGE. All denotations of female equivalents (fe) are based on the 200 µl final volume relative to the starting 200 females (*i.e.*, 1 fe/1 µl). *Cs*OPs were applied to cell overlays in PBS in a final volume of 100 µl.

Slide staining

Following the 60 min spreading period, cells were washed

with several volumes of PBS. Cells were fixed with 3.7% formaldehyde for 10 min, washed with several volumes of PBS and permeabilized with 100 µl of PBS + 0.2% Triton-X-100 for 10 min. Cells were washed with several volumes of PBS plus Triton-X and then double-stained for the actin cytoskeleton. Cells were incubated in 0.165 µM Alexa Fluor® 488 phalloidin (Molecular Probes), which is specific for F-actin, and 0.6 µM Alexa Fluor® 594 conjugated DNase-I (Molecular Probes), which binds specifically to G-actin, in 100 µl PBS for 30 min at room temperature. Cells were washed with several volumes of PBS, and the coverslip mounted in 1:1 glycerol/PBS and sealed with nail polish.

Microscopy and filter settings

Cells were observed on a Leica DMRE confocal microscope. The Alexa Fluor® 488 was excited at 488 nm and visualized using a 525/50 nm bandpass filter, and the Alexa Fluor® 594 DNase I excited at 568 nm and visualized using a 590 nm longpass filter. For spreading assays images were captured at 40 X. Each subject was recorded at 8 focal planes, from the plane of adherence to the coverslip to the top of the cell (~1.5 µm interval). The series image was combined using the Extended Focus function, which yields a single image composed of the brightest pixel value of the 8 focal planes for each X-Y value. For observations of G- and F-actin titers, images were collected at 100 X with a 50% pinhole diameter to reduce out of plane light, and a vertical stack of images at a 0.5 µm interval was captured from the plane of adherence to the top of the cell. Bias for under- and over-exposure was reduced at the time of image capture by verifying exposure using a gain-offset color lookup table (Glowovu in Leica TCS-NT), allowing some *a priori* standardization of background and image fluorescence.

Image analysis

Images were transferred to Image for PCs (Scion Corp., http://www.scioncorp.com) for analysis. For analysis of cell spreading, the FITC channel (F-actin) image was converted to a binary image with the THRESHOLD function and the mean and standard deviation of the pixel density of the entire image determined. Images then were corrected for background and daily variation in fluorescence by the application of a standard deviation correction: time course and plasma overlay images were standardized by application of the formula <<mean image pixel density – 2 x standard deviation of image pixel density>>, and *Cs*OP overlay images were standardized by <<mean image pixel density – 2.5 x standard deviation of image pixel density>> due to increased plasmatocyte density and greater F-actin heterogeneity. The image was converted to the DENSITY SLICE function, which permitted simultaneous automated outlining of cell perimeter and human confirmation of accuracy, and the threshold value (the value separating background from signal) was set equal to the result of the standard deviation correction above. The application of this correction effectively separated cells from the background, while not biasing the next step, tracing of the cell. Cell perimeter was determined by computer outlining of the cell, and each cell's area and perimeter was measured. Several control and treated images were analyzed by double blind observers to confirm reproducibility. The ratio of area to perimeter (A:P) is used often to describe the spreading of adherent cells, as cells that form many cytoplasmic processes have a reduced A:P ratio, while cells that remain circular have a high A:P ratio. We used a modified A:P statistic, roundness (Warren *et al.* 1996), to determine spreading ability (i.e., the relative number and morphology of cytoplasmic extensions). Roundness was determined using the formula <<Roundness=(400*π*Area)/(Perimeter^2)>>. This statistic has an advantage over other A:P ratios in that the value of cells with a low A:P ratio (irregular perimeter) approaches 0, while that of cells with a higher A:P ratio (regular perimeter) approaches 1. For each treatment and control dataset 20 images were drawn from 2 independent trials, which each consisted of 2 to 3 replicates.

For analysis of F- and G-actin levels, images were analyzed at 2 focal points, at the plane of adherence (z = 0 µm) and cytoplasm (z + 2.5 µm). Images were standardized as above with a transformation of 1.5 to avoid pixel saturation (<<mean density – 1.5 x standard deviation of density>>). The relative titers of both actin forms were defined as the mean pixel density of each cell at each focal point. The total relative actin in each cell was determined by multiplying the mean pixel density by cell area.

Statistical analyses

To account for daily variation in experiments (e.g. lepidopteran and parasitoid biology, fluorescence, and laser strength), all roundness data were analyzed and presented as ratios to the control for that day. For examination of F- and G-actin distribution and titer, the control data were analyzed and presented separately. As cell area is treatment-dependent, all total relative actin data are presented for trend only, and were not statistically analyzed. All remaining data were heteroscedastic and analyzed by ANOVA and then Games-Howell post-hoc test (Zar 1996). Significance is defined at a $\alpha = 0.05$.

Preliminary analyses of F- and G-actin images across parasitization showed consistent trends throughout the course of parasitization. Analyses therefore were confined to the first day post-parasitization.

Results

Correlation of F-actin cytoskeleton and hemocyte perimeter

To maximize data obtained from a single experiment, we sought to use the signal of fluorescently labeled phalloidin, which binds specifically to filamentous actin, to delineate the perimeter of hemocytes. Initial pilot assays visualized hemocytes isolated from both control (Fig. 1a-c) and parasitized (Fig. 1d-f) individuals by both phase contrast and epifluorescence. These observations verified that the F-actin cytoskeleton traced hemocyte outline precisely enough to use this technique as a proxy for plasma membrane perimeter in subsequent experiments.

Effect of Campoletis sonorensis parasitization on hemocyte spreading

Control hemocytes recognized and spread on glass coverslips, forming a large number of filopodia and in some cases lamellopodia (Fig. 2a). Parasitized cells both failed to adhere rapidly (data not shown) and failed to form lamellopodia and filopodia, resulting in the "rounded" morphology characteristic of unhealthy lepidopteran hemocytes (Fig. 1b).

Parasitization rapidly inhibited the ability of hemocytes to

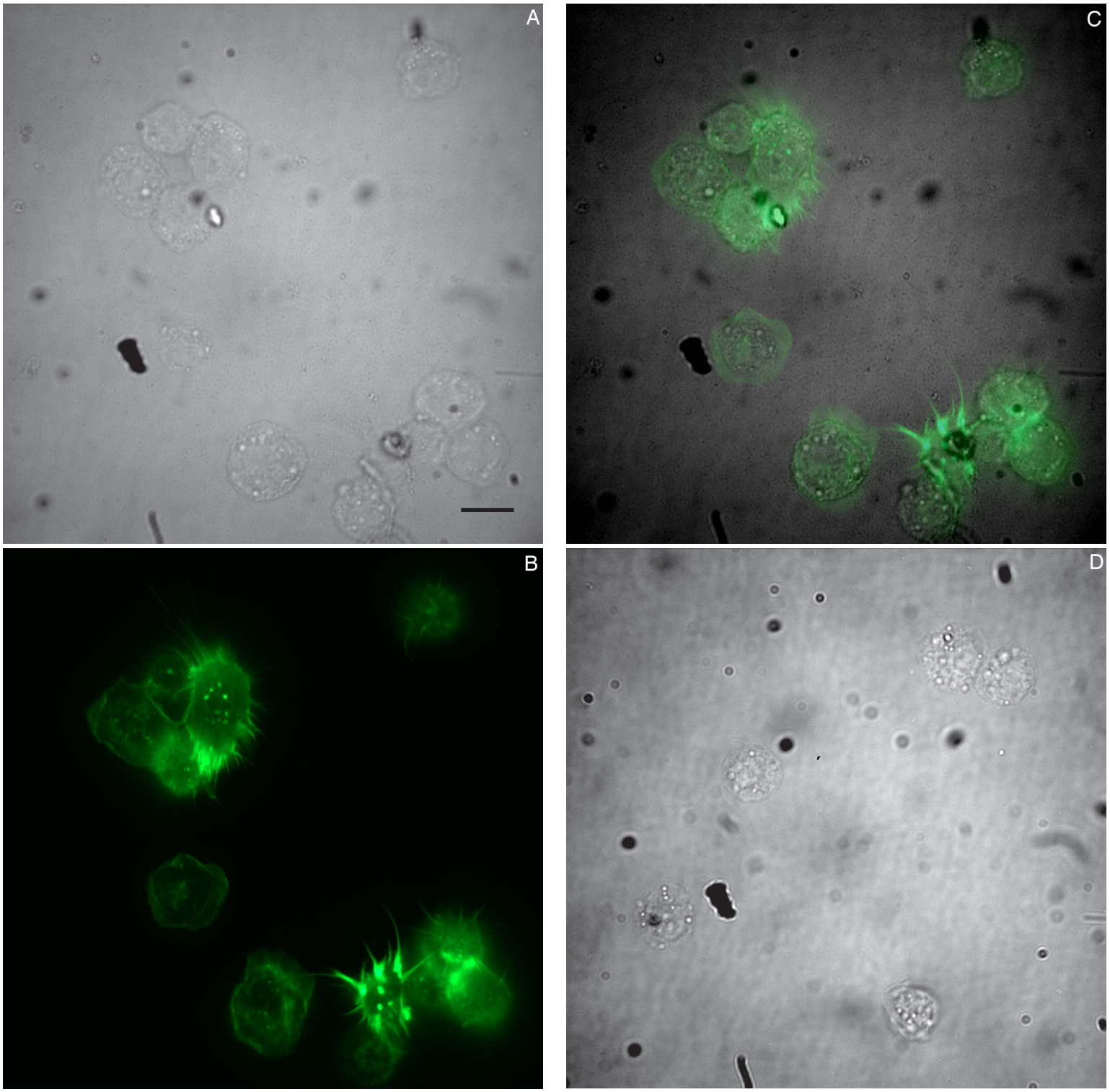

Figure 1. Correlation of hemocyte perimeter and FITC-phalloidin labeled F-actin cytoskeleton. (a-c) Control hemocytes were allowed to spread in PBS and visualized using (a) phase contrast and (b) FITC optics, and (c) phase and FITC images merged. (d-f) 2 day post-parasitized hemocytes allowed to spread in PBS and visualized using (d) phase contrast and (e) [page 5] FITC optics, and (f) [page 5] merged. Scale bar in (a): 10 µm.

spread (Fig. 3a). The multiple filopodia of control cells resulted in a well-spread cell with an irregular perimeter and thus a low roundness value (mean pooled control data: n = 678; area = 147.4 µm^2, SE = 9.44; perimeter = 80.17 µm, SE = 5.59; roundness 39.44, SE = 0.84). By 3 h post parasitiation (pp) cells exhibited a reduction in spreading ability, with reduced area and perimeter relative to control resulting in an increased roundness value (t_{3hctl} : $t_{3hpp\ ttest(2),\ 138}$, p<0.001). Spreading ability was depressed throughout infection, with no significant return in spreading as late as 7 d pp as shown by *t*-test of control versus parasitized hemocytes at each

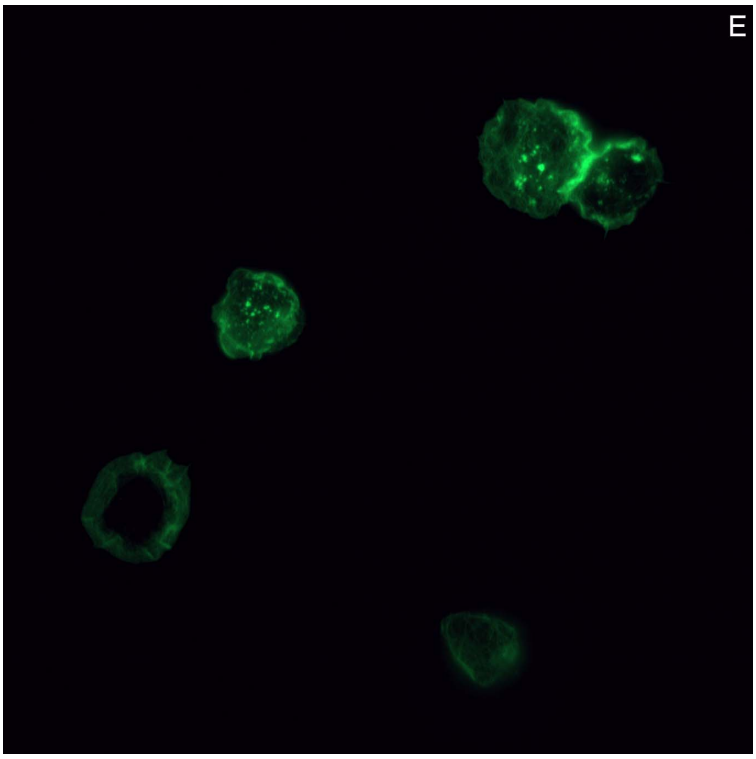

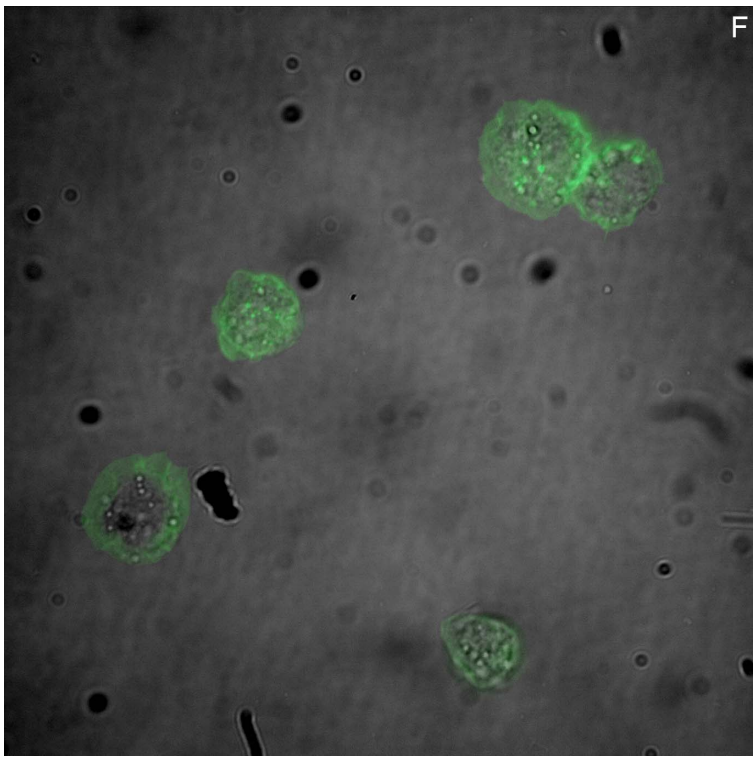

Figure 1. (e-f) See legend on page 4.

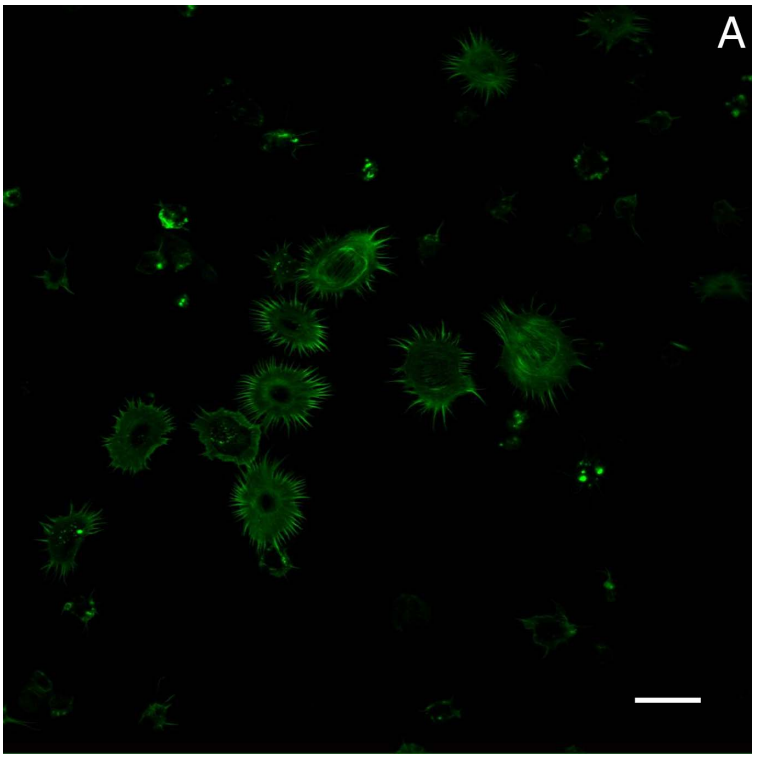

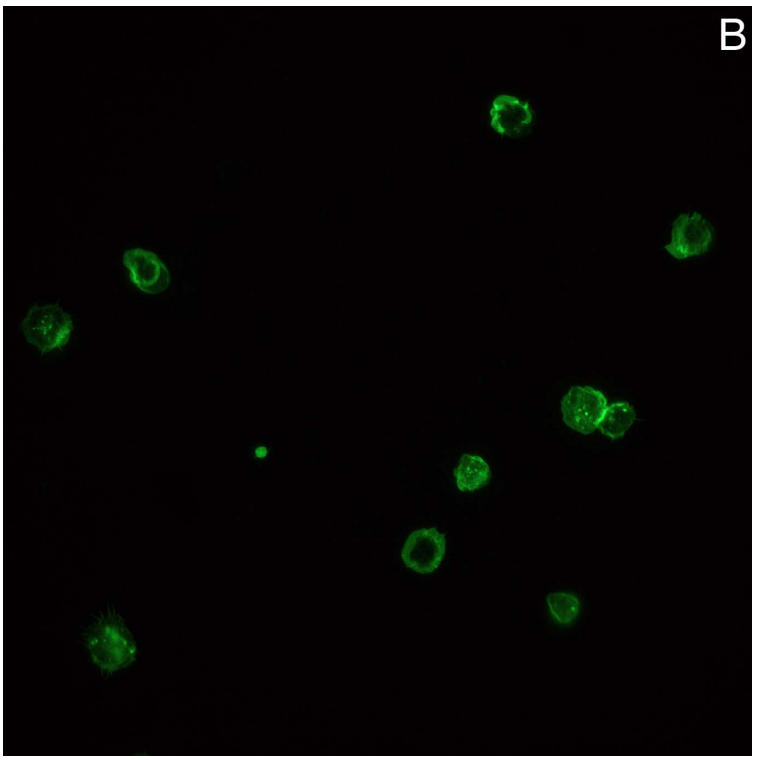

Figure 2. Morphology of adherent hemocytes. (a) Control hemocytes spread in PBS. (b) Hemocytes from *Heliothis virescens* three days after parasitization, spread in PBS. (c) [page 6] Control hemocytes spread in plasma isolated from control *H. virescens*. (d) [page 6] Control hemocytes spread in plasma isolated from *H. virescens* three days after parasitization. (e) [page 6] Control hemocytes spread in the presence of 1.0 female equivalents of *Campoletis sonorensis* ovarian proteins. Scale bar in (a): 20 μm.

time point (Fig. 3a). When roundness was standardized across time points by dividing the parasitized roundness value for each cell by the mean roundness of the control cells, regression found no significant relationship between degree of roundness and time after parasitization ($y = 1.72x + 39.95$, $r^2 = 0.119$). Observation of the focal depth of cells suggested that spreading and focal depth were inversely correlated, leading to some maintenance of cell volume, although the data were not quantified.

Effect of hemolymph factors on hemocyte spreading

Control cells formed an increased number of cytoplasmic

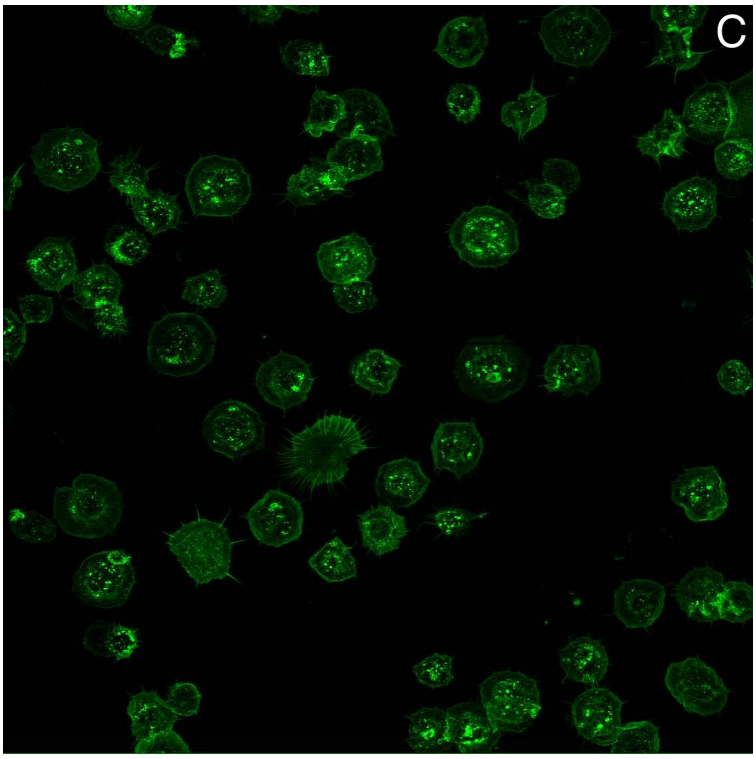

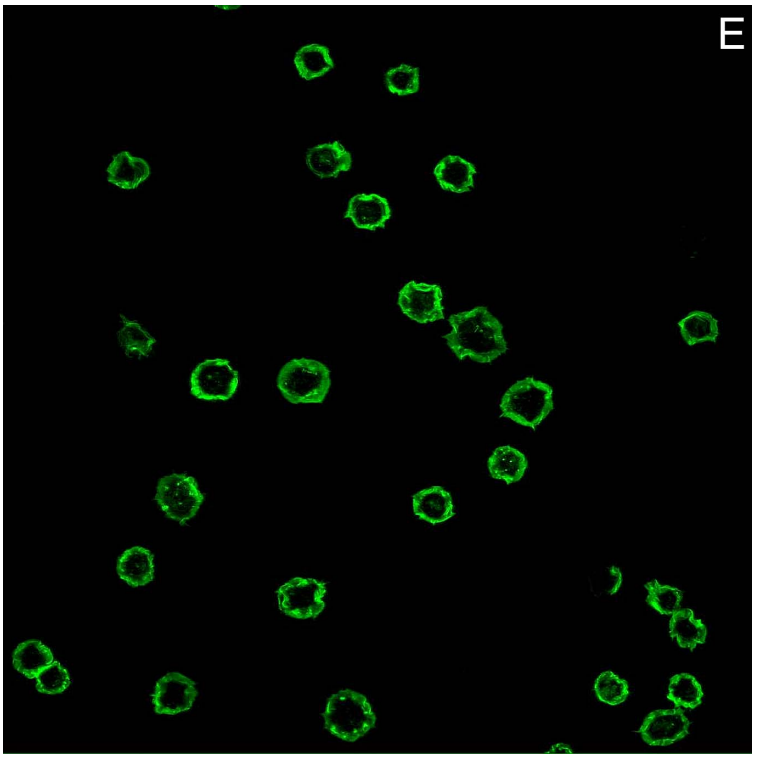

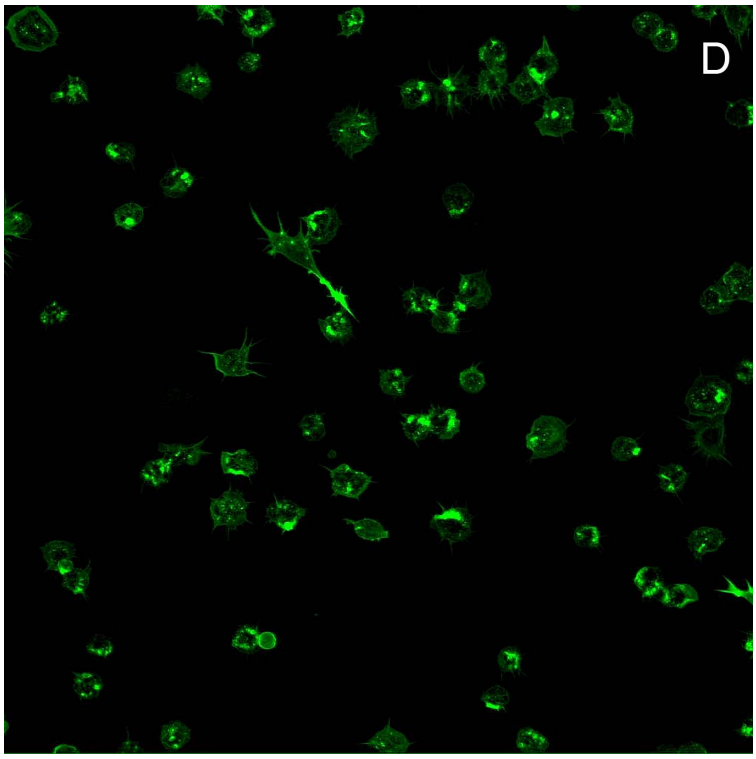

Figure 2. (c-e) See legend on page 5.

processes when allowed to spread in the presence of plasma of other control caterpillars rather than PBS (Fig. 2c). Cells overlaid with plasma from parasitized individuals had an intermediate number of filopodia, with fewer than those overlaid with plasma from control larvae but more than parasitized individuals from the same time point post-parasitization (Fig. 2d). The increased number of processes, and thus increased perimeter of the cells allowed to spread in the presence of plasma, led to an overall reduction of roundness relative to their controls (Fig. 3b). The differences were significant, with a general increase in spreading ability in the order parasitized – parasitized plasma – control plasma – PBS, suggesting activation of hemocytes by plasma components.

Effect of Campoletis sonorensis ovarian proteins on hemocyte spreading

The number of filopodia extended during spreading by cells overlaid with *Cs*OPs was reduced (Fig. 2e) as compared to both PBS and sucrose dialyzed to PBS controls. The mean cell area and perimeter were reduced at concentrations of *Cs*OPs as low as 0.5 female equivalents (fe), the lowest value assayed, with concommitant significant increases in roundness ($t_{ctl} : t_{0.5fe\ ttest(2),\ 267}$, p=0.020). *Cs*OP effect on cell spreading appeared concentration dependent (Fig. 4) though linear regression failed to exhibit statistical significance, presumably due to large variance ($y = 1.9768\ x + 47.56$, $r^2 = 0.04$). As with parasitized cells, reduced spreading was correlated with an increased z-axis dimension of the cells, indicating some maintenance of cell volume.

Observations on actin cytoskeletal pathologies

Serial reconstructions of whole cells revealed different distributions and overall fluorescence (i.e. concentration) of both monomeric and filamentous actin, not just filamentous as had been previously reported (Webb and Luckhart 1994) (Fig. 5). F-actin stress fibers were discernable in control hemocytes and rings were rarely observed, yielding a heterogeneous distribution, while G-actin colocalized in many cases with F-actin at the plane of adhesion and

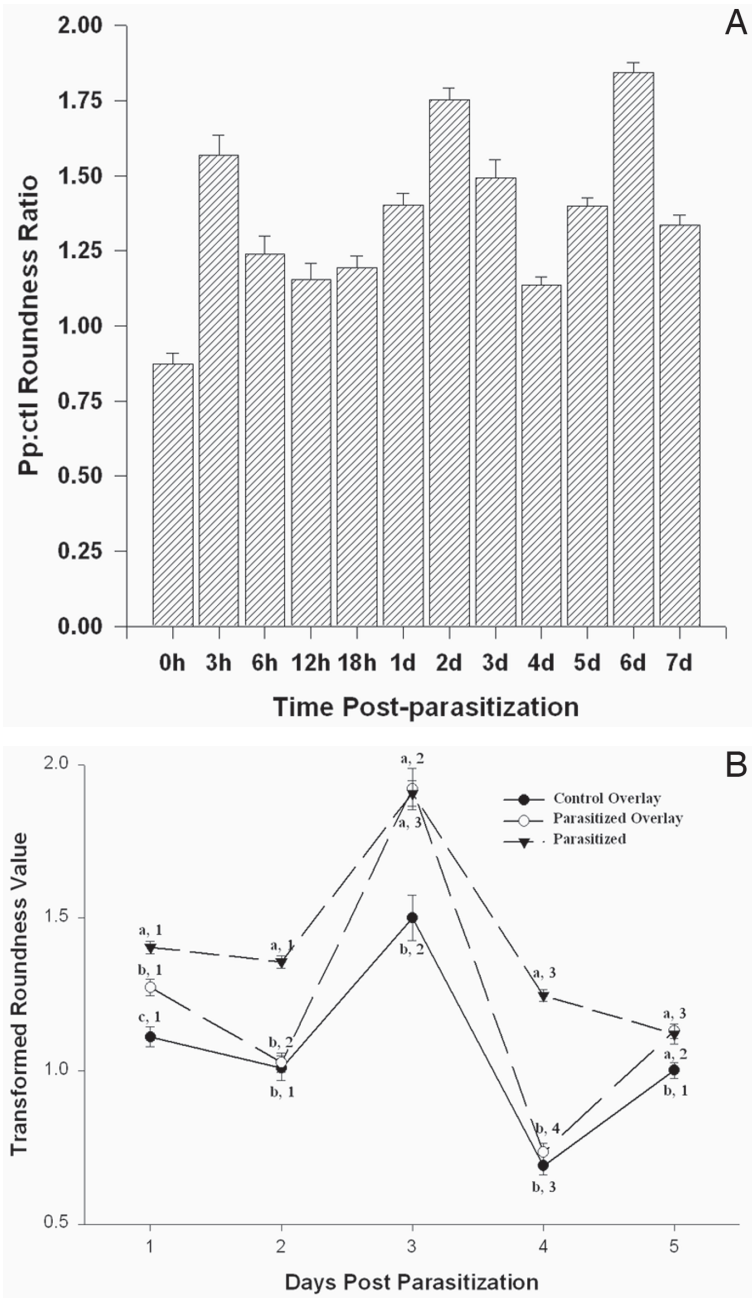

Figure 3. Mean roundness of cells at various time points post-parasitization (pp) as compared to control (ctl). (a) Ratio of parasitized cells' roundness to control (pp/ctl) at time points after parasitization; error bars are standard error of the mean. (b) Transformed roundness (treatment:control) of hemocytes isolated from control or parasitized *Heliothis virescens* allowed to spread in the presence of various media. Error bars are standard errors, different lettered superscripts indicate mean transformed roundnesses differ between treatments at the same time point at α=0.05 by Games-Howell post-hoc analysis and different numbered superscripts indicate mean transformed roundness differs between time points within the treatment group at α=0.05

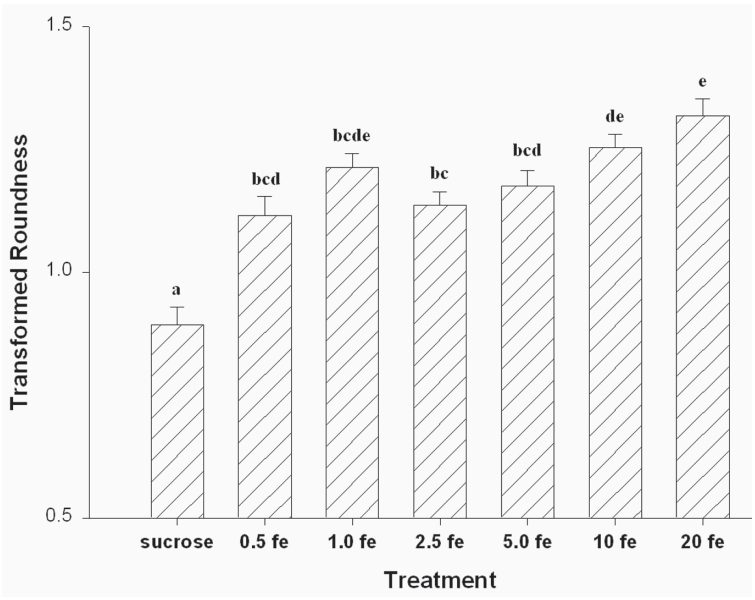

Figure 4. Mean roundness of cells overlaid with *Cs*OPs. Hemocytes were isolated from control 3rd instar *Heliothis virescens* and allowed to spread for 1 hr in PBS, sucrose (negative control of sucrose from sucrose gradient ovarian protein isolation, dialyzed to PBS), or increasing female equivalents (fe) of *Campoletis sonorensis* ovarian proteins in PBS. The sucrose and *Cs*OP overlays were standardized by dividing each roundness value by the mean control roundness (see Fig. 3a). Error bars represent the mean transformed roundness of the cells, and error bars show the standard errors of the mean. Same superscript letter above the bar indicates means are not significantly different at α=0.05.

more homogeneously elsewhere (Fig. 5a-f). FITC-phalloidin was distributed homogeneously throughout the cytoplasm of cells from parasitized individuals, though peripheral F-actin rings were consistently observed (Fig. 5g-l). G-actin was homogeneously distributed, colocalizing with the F-actin cytoskeleton, although there were more punctate foci of G-actin, in the absence of dense F-actin, in parasitized cells than control. The actin cytoskeleton in overlaid cells typically mirrored the results of the spreading assay, as both F- and G-actin were distributed in control overlays as in control cells, and both forms distributed to an intermediate degree between parasitized and control cells in cells overlaid with plasma from parasitized larvae.

Quantitation of actin distribution and titers

The mean density of F-actin (sum of mean fluorescence value at each X-Y pixel divided by the area of fluorescence of the cell) is a function of actin concentration at a given X-Y pixel value, so we used density as an indicator of actin concentration. Mean density of FITC-phalloidin fluorescence at the plane of adherence was significantly reduced in hemocytes isolated from parasitized individuals relative to control, and was increased in cells overlaid with plasma (Fig. 6a). Mean cytoplasmic F-actin density was also altered by treatment, with control cells in PBS exhibiting the greatest density (Fig. 6a).

The mean density of G-actin at the plane of adherence increased in cells from individuals 1 day after parasitization relative to control individuals, and statistically similar levels were observed in all four-treatment groups (Fig. 6b). The distribution of G-actin between plane of adherence and cytoplasm was inversely related, as the treatments with the highest mean G-actin density at the plane of adherence had the lowest cytoplasmic density (Fig. 6b). The pattern mirrored cytoplasmic F-actin levels, further correlating co-

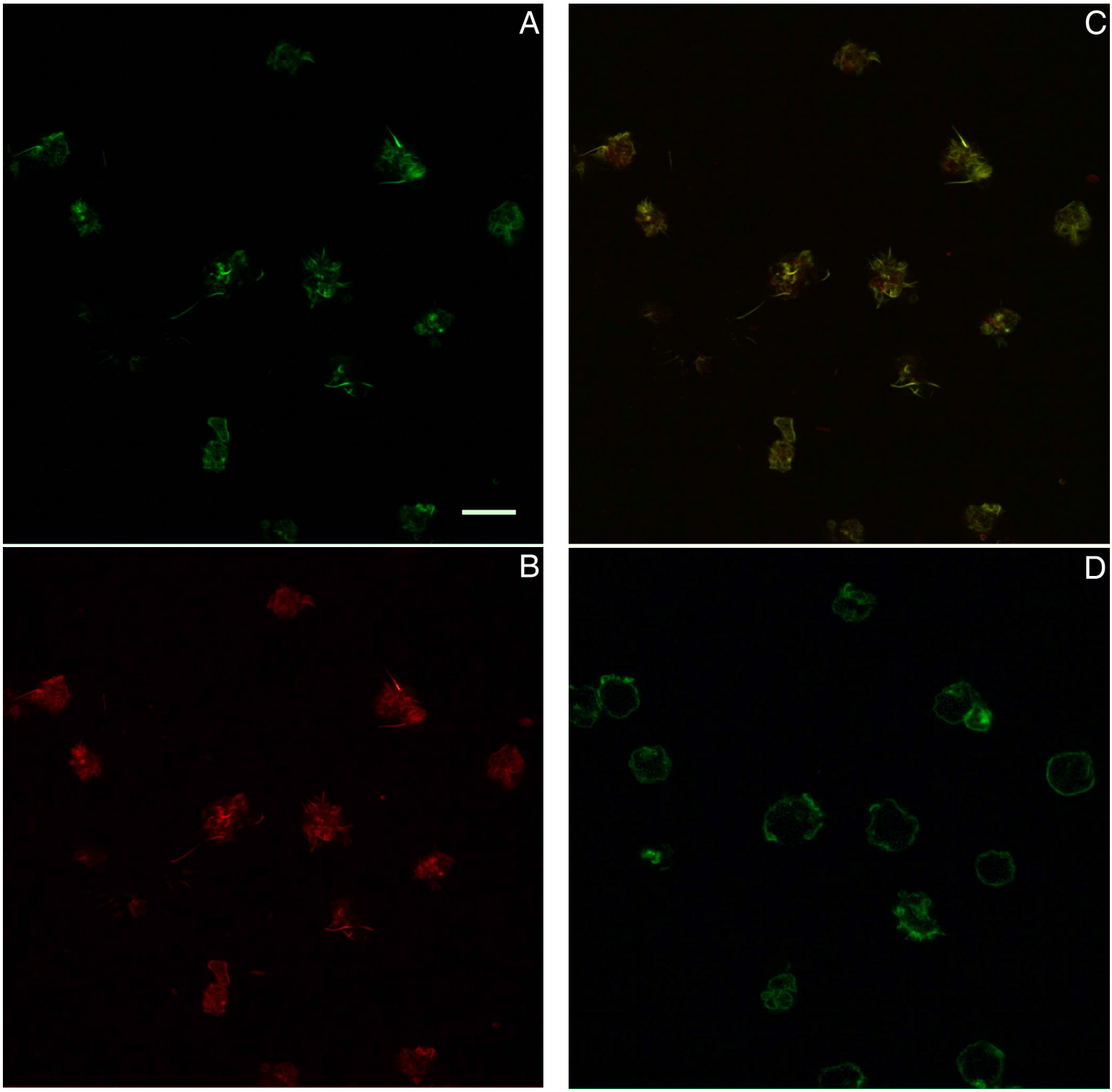

Figure 5. Images of F- and G-actin distribution in control and parasitized hemocytes at two focal points. *Heliothis virescens* hemocytes were allowed to spread for 1 hr in PBS and stained for F-actin (green) and G-actin (red). (a-c) Control hemocytes at the plane of adherence (z), and (d-f) at z+2.5 µm. (g-i) Hemocytes from a 1 d post-parasitized *H. virescens* at z and at (j-l) z+2.5 µm. Scale bar in (a): 10 µm

localization of the two-actin forms.

Different F-actin:G-actin ratios between treatments and focal distances can be indicative of a shift from one form to the other. If this is assumed to be the case here, then the F-actin to G-actin ratio at the plane of adherence suggests a shift from F-actin to G-actin in hemocytes 1 day after parasitization (Fig. 7), while the other three treatments had an F-:G-actin ratio>1. The cytoplasmic F-:G-actin ratio was reduced in hemocytes 1 day after parasitization, a significant reduction relative to the control and control overlay treatments.

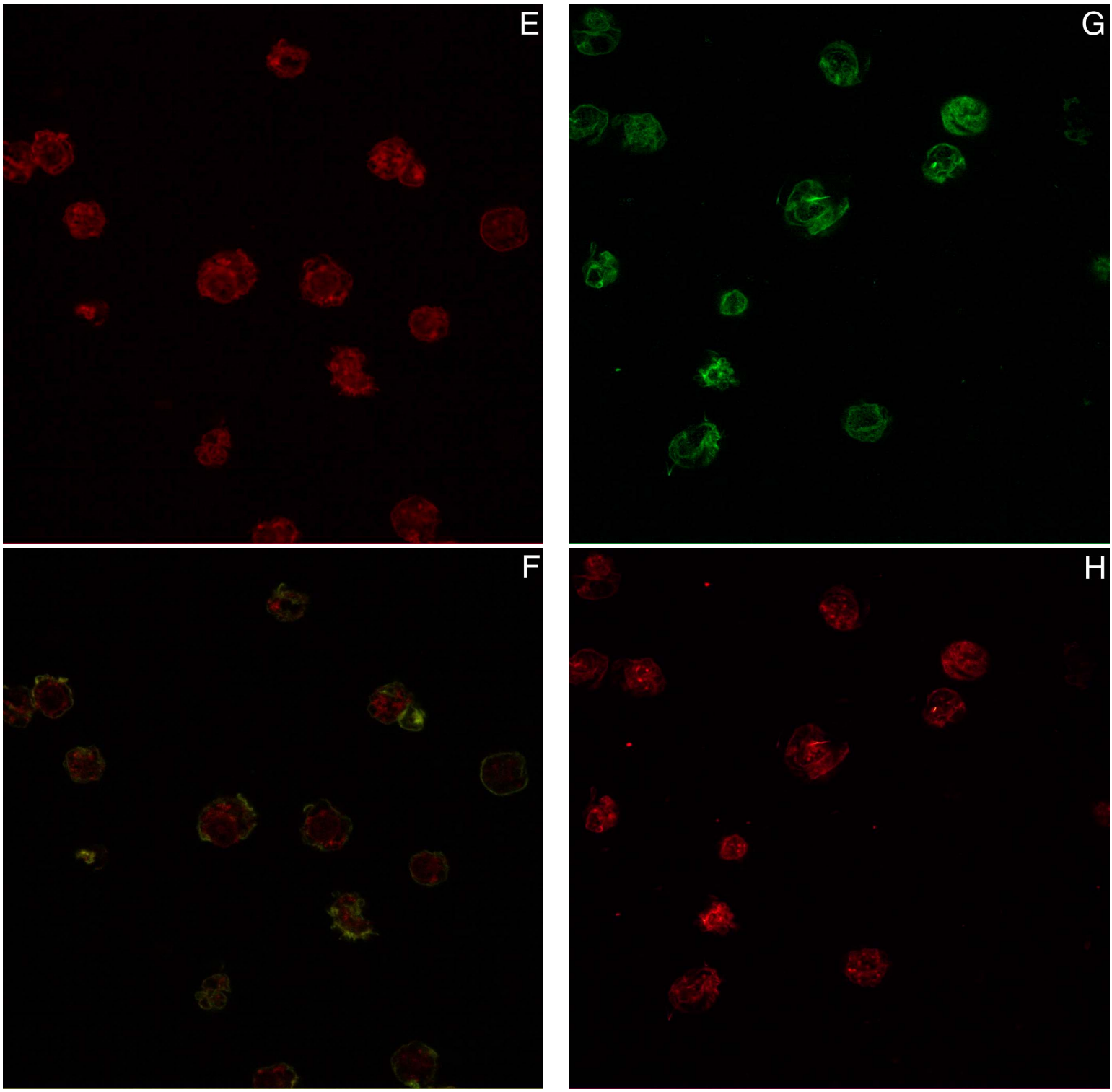

Figure 5 [Continued from page 8]. Images of F- and G-actin distribution in control and parasitized hemocytes at two focal points. *Heliothis virescens* hemocytes were allowed to spread for 1 hr in PBS and stained for F-actin (green) and G-actin (red). (a-c) Control hemocytes at the plane of adherence (z), and (d-f) at z+2.5 µm. (g-i) Hemocytes from a 1 d post-parasitized *H. virescens* at z and at (j-l) z+2.5 µm. Scale bar in (a): 10 µm

The total F-actin and G-actin titer, as determined by <<mean density of fluorescence x area of fluorescence per cell>>, was determined at both focal distances. Overall, there was a reduction in F-actin in cells 1 day after parasitization relative to control and overlay treatments at the plane of adherence, with an increase in F-actin for both overlays relative to control (Fig. 8a). F-actin levels were inversely related with an overall reduction in cytoplasmic F-actin observed in the overlay treatments. This measurement is biased due to increased cell area, but the mean density of FITC-phalloidin fluorescence was significantly increased in the overlays relative to

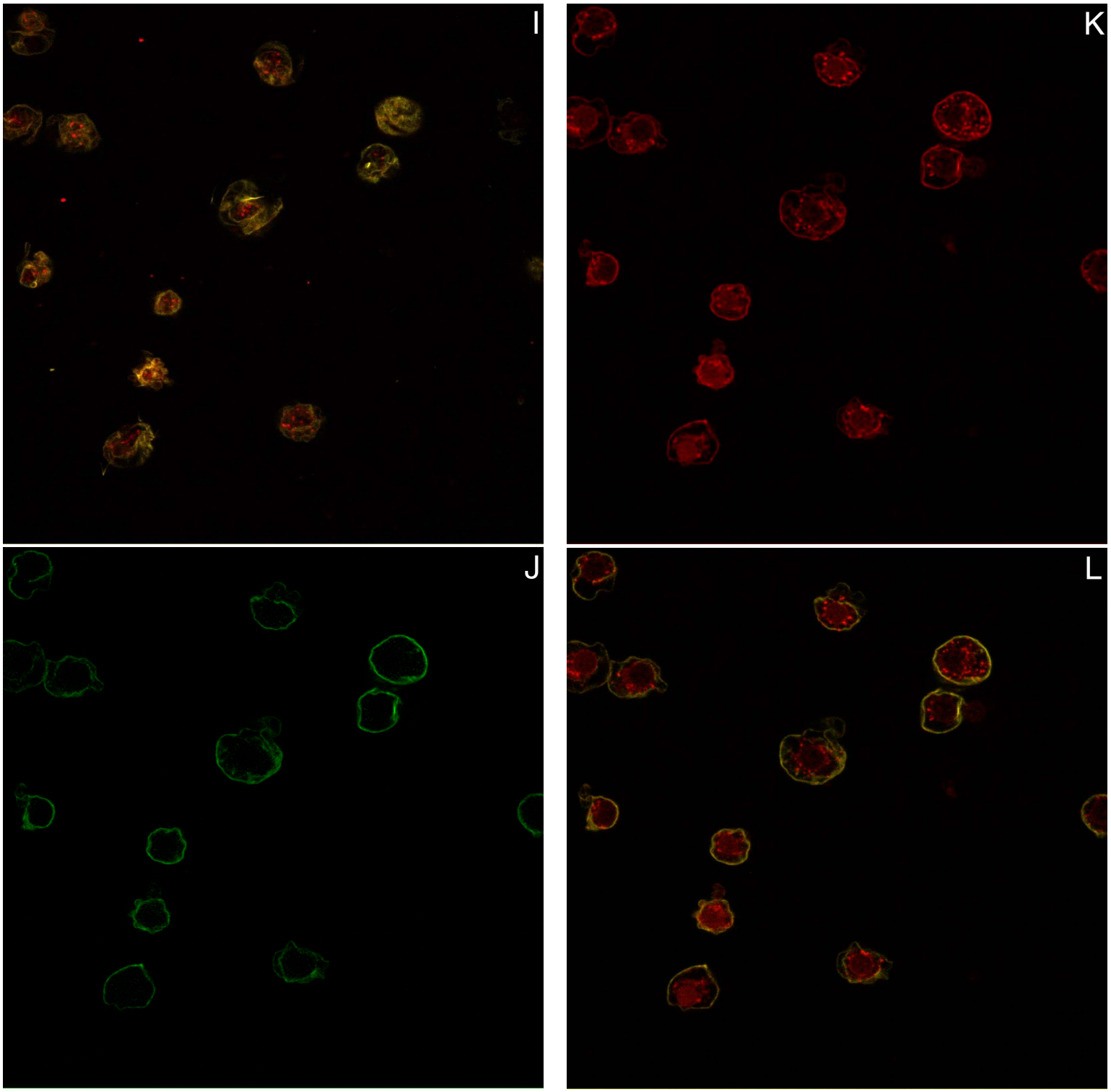

Figure 5 [Continued from page 8]. Images of F- and G-actin distribution in control and parasitized hemocytes at two focal points. *Heliothis virescens* hemocytes were allowed to spread for 1 hr in PBS and stained for F-actin (green) and G-actin (red). (a-c) Control hemocytes at the plane of adherence (z), and (d-f) at z+2.5 µm. (g-i) Hemocytes from a 1 d post-parasitized *H. virescens* at z and at (j-l) z+2.5 µm. Scale bar in (a): 10 µm

parasitized, though less than the control (data not shown), further supporting that F-actin is reduced at the plane of adherence in parasitized cells and increased in the overlays. G-actin content was reduced in the parasitized hemocytes, but increased in the overlay treatments (Fig. 8b). In particular there was a greater amount of G-actin at the plane of adherence in the overlaid cells. This affected the overall distribution of cellular actin, as there was an increase in actin present at the plane of adherence in the overlay treatments relative to both control and 1 day after parasitization (Fig. 8c). Cytoplasmic levels of actin were altered, with the lowest titer present

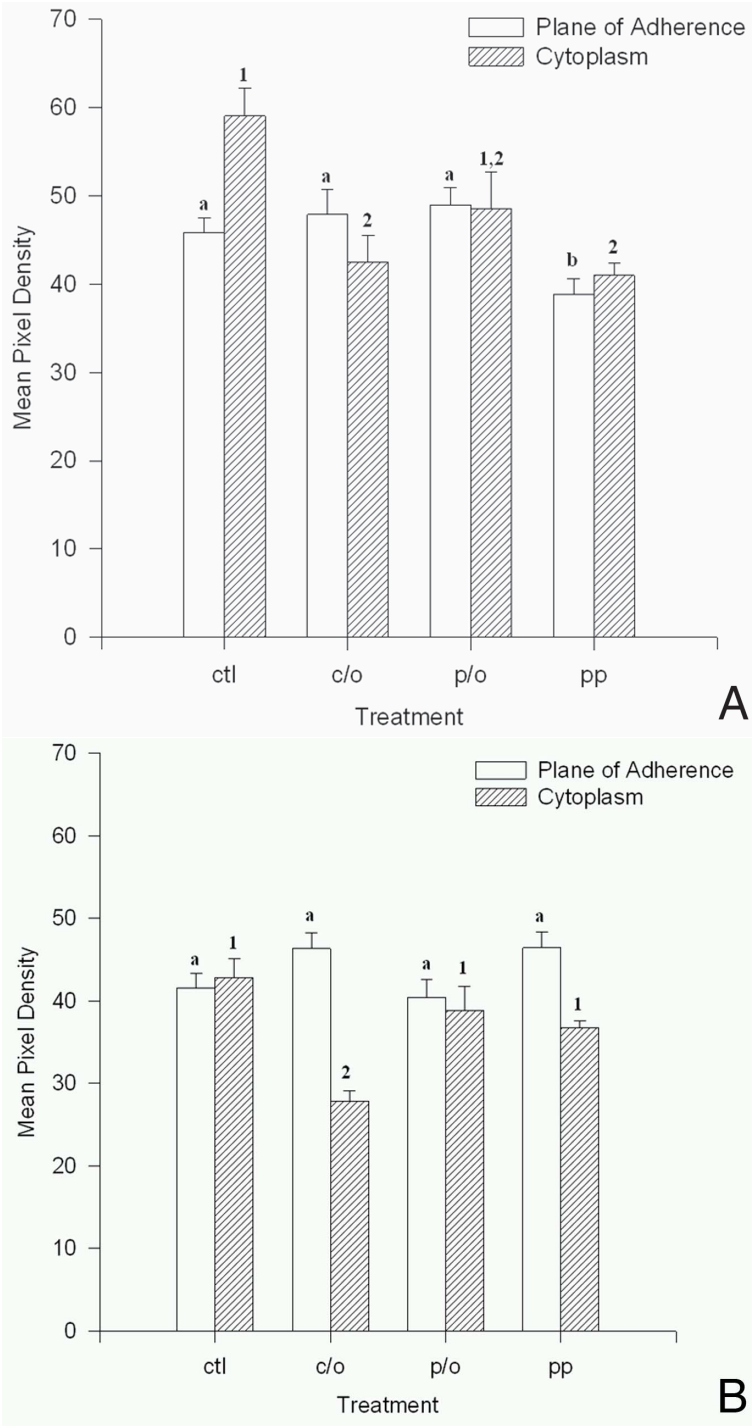

Figure 6. Mean relative distribution and density of actin in *Heliothis virescens* hemocytes as measured by fluorescence. Hemocytes from control individuals were allowed to spread in PBS (ctl) or plasma from control (c/o) or larvae one day after parasitization (p/o), or were isolated from larvae one day after parasitization and allowed to spread in PBS (pp). Images were captured using (a) FITC and (b) rhodamine optics at or near the plane of adherence to the coverslip (z) and at z+2.5µm (cytoplasm). Error bars show standard errors of the mean. Different letters above bars indicate means are statistically different at z-focal distance at α=0.05, different numbers above bars indicate significant difference at z+2.5µm.

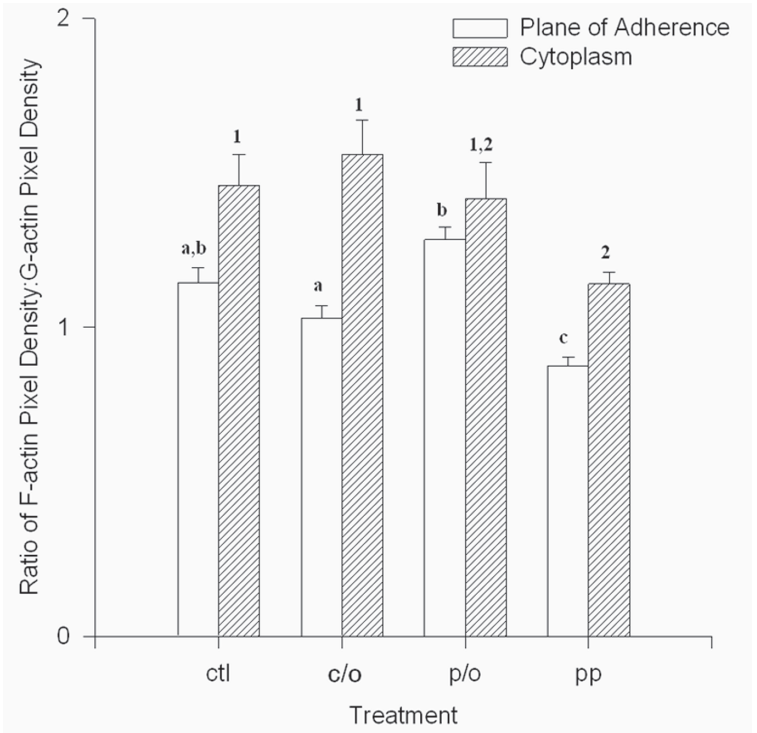

Figure 7. F-:G-actin ratio in *Heliothis virescens* hemoctyes. The ratio was determined by comparison of mean density of FITC-phalloidin staining to DNase I-rhodamine staining on a per cell basis at two focal distances in four treatment groups (see Fig. 6). Error bars are standard error of the mean, and different letters (z) and numbers (z+2.5µm) indicate means significantly differ at that focal distance at α=0.05.

in control cells overlaid with plasma from larvae 1 day after parasitization. Overall, there was a trend to reduction in total actin in cells from larvae 1 day after parasitization, while an increase was observed in cells overlaid with plasma from both control and parasitized larvae (Fig. 8d).

Discussion

The primary immune response of arthropods to metazoan parasites is hemocytic encapsulation, a highly organized and coordinated reaction involving multiple hemocyte types, primarily granulocytes and plasmatocytes. Encapsulation is regulated by chemical (Clark *et al.* 1997) and tactile (Strand and Clark 1999) cues, both of which involve the actin cytoskeleton. Previous studies have shown that maternal factors introduced during parasitization, such as venom (Wago and Kitano 1985) and ovarian proteins (Webb and Luckhart 1994), can lead to alterations in the F-actin cytoskeleton resembling those observed during cytochalasin-D treatment, as might some larval parasitoid-associated factors (Beckage 1993). Polydnaviruses commonly induce F-actin disruption, although they generally do not share genes (Webb *et al.*, in prep.), and likely are unrelated (Turnbull and Webb 2002). This suggests that polydnaviruses have evolved multiple methods with which to attack the cytoskeleton and disrupt immunity. A mechanistic difference is further supported by the observation that *Cs*IV does not require direct infection of hemocytes, as secreted proteins can induce some of the pathologies observed (Li and Webb 1994; Luckhart and Webb 1996). However, *Microplitis demolitor* Bracovirus requires direct

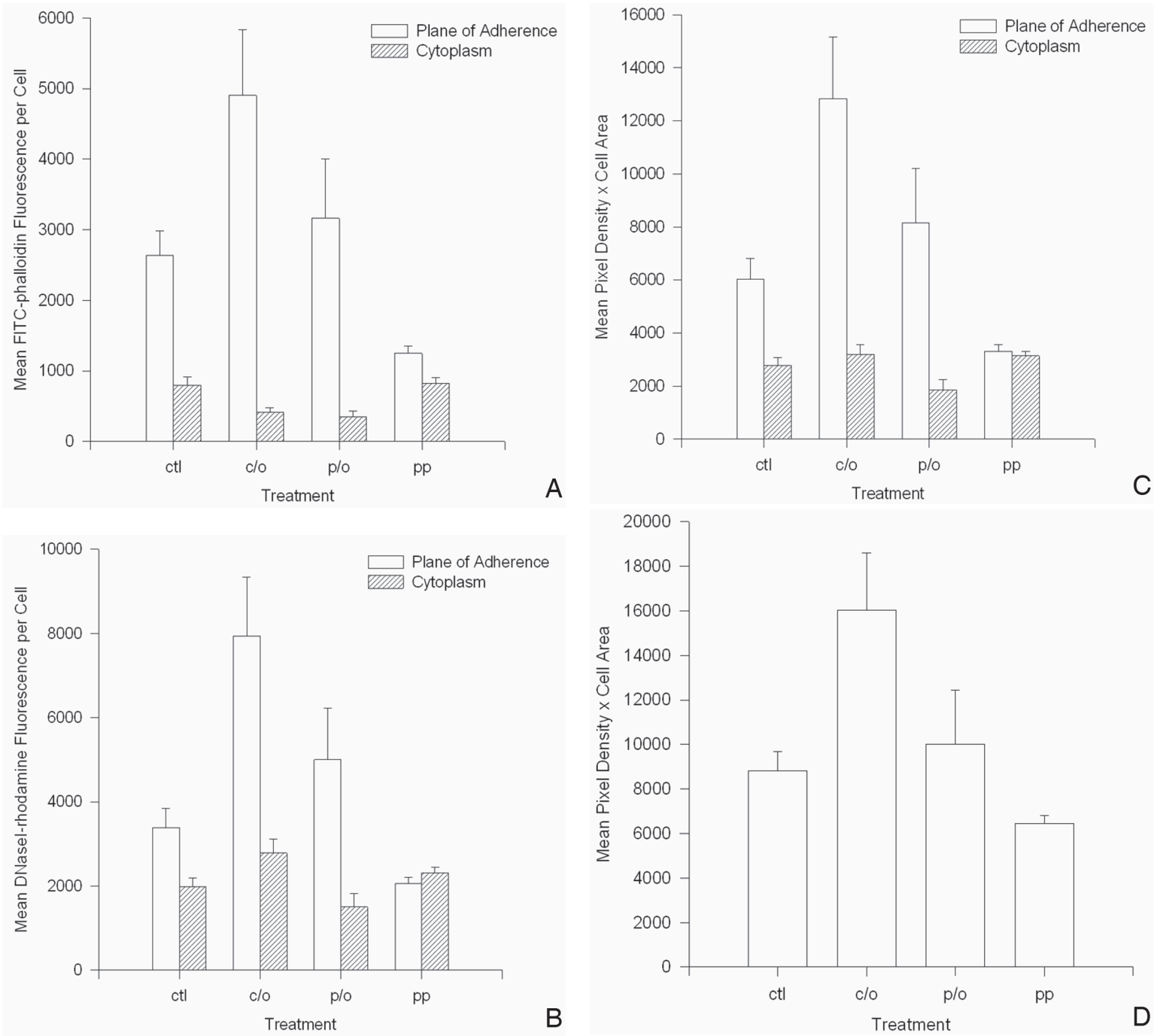

Figure 8. Actin content in *Heliothis virescens* hemocytes. Treatment groups and focal distances are the same as in Fig. 6. See Methods for determination of total actin content. (a) Total F-actin. (b) Total G-actin. (c) Total actin at each focal distance. (d) Summed actin content.

infection of hemocytes (Strand 1994; Strand and Pech 1995; Trudeau *et al.* 2000), suggesting the lack of secreted proteins and interaction with different target molecules.

In agreement with previous reports, we found that the F-actin cytoskeleton was disrupted in hemocytes from parasitized individuals and control hemocytes treated with parastization-associated factors. As in previous findings, few stress fibers were observed. We did observe F-actin foci, primarily in focal adhesions and skirts. Most interesting is that we have for the first time demonstrated that there is a reduced complement of F-actin. Our findings suggest that some polymerization does occur in virus-infected cells, although it is likely an aberration. Previously, the F-actin pathology in hemocytes following parasitization has been thought to represent an increased depolymerization of F-actin. However, our data suggest that this is not the only cause of low F-actin levels, as there may be a reduction in actin synthesis or increase in actin breakdown.

G-actin titers were greater in total but not density in control

and overlay treatments relative to parasitized cells. The lack of change in density suggests that there was no alteration in distribution in any of the treatments, while the titer increase is likely due to the increased area of the control and overlay cells relative to the parasitized cells. The pattern and titer of G-actin is of interest, as it was demonstrated previously that G-actin levels decrease during phagocytosis in cockroach hemocytes due to filamentization (Gupta and Campenot 1996). The concomitant decrease in both total titer of F- and G-actin and the F-actin:G-actin ratio in parasitized cells, particularly at the plane of adherence, support reduced synthesis or increased breakdown of cellular actin. Additionally, the reduced effects on actin observed in the parasitized overlay treatments relative to their parasitized controls suggest the role of nonsecreted *Cs*IV gene products in inducing these changes.

It therefore appears that *Cs*IV affects the total actin pool of hemocytes, disrupting hemocyte capacity for immune response, rather than only through depolymerization of F-actin as has been previously suggested (Asgari *et al.* 1997; Webb and Luckhart 1994). This may occur through post-transcriptional inhibition, a particularly attractive hypothesis as *Cs*IV-infection inhibits translation of specific transcripts (Shelby and Webb 1997; Shelby *et al.* 1998). Analysis of F-actin transcription and translation patterns in hemocytes during challenge with individual viral proteins is now possible due to the recent development of *in vitro* techniques for the study of hemocytes (Beck and Strand 2003) in combination with recombinant viral proteins (Li and Webb 1994; Soldevila *et al.* 1997). Conceptually, viral proteins such as the cys-motif proteins may inhibit actin translation in hemocytes. This would lead to reduced F-actin, adhesion, and motility, eventually inhibiting encapsulation responses. Alteration of F-actin also is likely to inhibit cytokine release, reducing the immune responsiveness of uninfected hemocytes.

The assays used in our experiments were designed to facilitate the determination of the effects of specific virus-encoded proteins on hemocytes, allowing clarification of their roles in host susceptibility. *In vivo* effects likely are greater than those observed here, as the most severely affected hemocytes do not adhere to slides and hence were not quantified in our assays. Nevertheless the cells examined exhibit a reproducible phenotype, enabling a sensitive *in vitro* assay. The assays demonstrate that there is an interaction occurring between cytokines and nonsecreted virus products, leading to incomplete inhibition of spreading in control cells overlaid with parasitized plasma. The similarity of the parasitized and control overlay treatment results suggests that cells in the former group are capable of receiving and reacting to plasma-borne chemicals such as cytokines. Secreted viral proteins therefore do not abolish cytokine release and/or uptake and response, although reduced ability to spread relative to control overlays does imply that secreted proteins induce some hemocyte pathologies. One hemocyte pathology that these assays do not address is apoptosis, which is induced by *Cs*IV infection (Webb and Strand, unpublished observations) and is an important component of antiviral defense (Clarke and Clem 2003; Clem 2001). Propidium iodide staining of cells overlaid with parasitized plasma does not support induction of apoptosis by secreted proteins (Turnbull, personal observation), but it remains to be shown definitively whether secreted, intracellular, or both sets of virus-encoded proteins induce apoptosis.

We have shown that the spreading ability of hemocytes isolated from *H. virescens* parasitized by the ichneumonid *C. sonorensis* is reduced, in agreement with previously obtained reports (Davies *et al.* 1987; Prévost *et al.* 1990). However, our results also show that control hemocytes respond to parasitization-associated factors *in vitro*, although the rounding pathology is less severe than that induced by parasitization. The intermediate state of overlaid cells suggests that there are intracellular factors, in addition to hemolymph-born *Cs*OPs and cys-motif proteins, affecting the actin cytoskeleton. We have associated the observed rounding with reduction of cellular actin content, suggesting that it may be due to inhibition of actin translation accompanying *Cs*IV infection. F-actin distribution is altered, and the rate of filamentization may be reduced by lowered total cellular actin. Effects on the F-actin cytoskeleton likely impair degranulation, and reduce responsiveness of granulocytes to infection, as well as cytokine release. Such effects would reduce recruitment of plasmatocytes by altering actin based endocytic and pinocytic pathways and lessening motility. Establishing that the hemocyte morphology assays are useful for specific cell populations and *in vitro* hemocyte assays will allow bioassay of individual virus proteins and begin the process of associating pathologies with specific polydnavirus proteins. Combination of these microscopic methods with molecular (transcription level) and biochemical (actin turnover) assays will allow quantification of the effects of specific parasitization-associated factors, including venom, ovarian proteins, and individual viral genes, to elucidate their roles in disruption of cellular immunity.

Acknowledgements

We would like to thank Drs. Robin Cooper, Roland Hilgarth, and Anne-Nathalie Volkoff for helpful suggestions. The work presented in this paper was partially supported by grants from the National Science Foundation to BAW and an REU supplement to SBM. This manuscript is publication 03-08-151 of the Kentucky Experiment Station.

References

Albrecht U, Wyler T, Pfister-Wilhelm R, Gruber A, Stettler P, Heiniger P, Kurt E, Schumperli D, Lanzrein B. 1994. Polydnavirus of the parasitic wasp *Chelonus inanitus* (Braconidae): characterization, genome organization and time point of replication. *Journal of General Virology* 75: 3353-3363.

Asgari S, Schmidt O, Theopold U. 1997. A polydnavirus-encoded protein of an endoparasitoid wasp is an immune suppressor. *Journal of General Virology* 78: 3061-3070.

Beck M, Strand MR. 2003. RNA interference silences *Microplitis demolitor* Bracovirus genes and implicates *glc1.8* in blocking adhesion of infected host cells. *Virology* 314: 521-535.

Beckage NE. 1993 in *Parasites and Pathogens of Insects* (Beckage NE, Thompson SN, Federici BA, eds) Vol. 1, pp. 25-58, 2 vols., Academic Press, N.Y.

Blissard GW, Vinson SB, Summers MD. 1986. Identification, mapping and *in vitro* translation of *Campoletis sonorensis* virus mRNAs from parasitized *Heliothis virescens* larvae.

Journal of Virology 57: 318-327.

Clark KD, Pech LL, Strand MR. 1997. Isolation and identification of a plasmatocyte-spreading peptide from the hemolymph of the lepidopteran insect *Pseudoplusia includens*. *Journal of Biological Chemistry* 272: 23440-23447.

Clark KD, Witherell A, Strand MR. 1998. Plasmatocyte spreading peptide is encoded by an mRNA differentially expressed in tissues of the moth *Pseudoplusia includens*. *Biochemical and Biophysical Research Communication* 250: 479-485.

Clarke TE, Clem RJ. 2003. In vivo induction of apoptosis correlating with reduced infectivity during baculovirus infection. *Journal of Virology* 77: 2227-2232.

Clem RJ. 2001. Baculoviruses and apoptosis: the good, the bad, and the ugly. *Cell Death and Differentiation* 8: 137-143.

Cui L, Webb BA. 1996. Isolation and characterization of a member of the cysteine-rich gene family from *Campoletis sonorensis* polydnavirus. *Journal of General Virology* 77: 797-809.

Cui L, Soldevila A, Webb BA. 1997. Expression and hemocyte-targeting of a *Campoletis sonorensis* polydnavirus cysteine-rich gene in *Heliothis virescens* larvae. *Archives of Insect Biochemistry and Physiology* 36: 251-271.

Cui L, Soldevila AI, Webb BA. 2000. Relationships between polydnavirus gene expression and host range of the parasitoid wasp *Campoletis sonorensis*. *Journal of Insect Physiology* 46: 1397-1407.

Cusson M, Laforge M, Miller D, Cloutier C, Stoltz D. 2000. Functional significance of parasitism-induced suppression of juvenile hormone esterase activity in developmentally delayed *Choristoneura fumiferana* larvae. *General and Comparative Endocrinology* 117: 343-354.

Davies DH, Strand MR, Vinson SB. 1987. Changes in differential haemocyte count and *in vitro* behaviour of plasmatocytes from host *Heliothis virescens* caused by *Campoletis sonorensis* Polydnavirus. *Journal of Insect Physiology* 33: 143-153.

Dib-Hajj SD, Webb BA, Summers MD. 1993. Structure and evolutionary implications of a "cysteine-rich" *Campoletis sonorensis* polydnavirus gene family. *Proceedings of the National Academy of Science, U.S.A.* 90: 3765-3769.

Gardiner EM, Strand MR. 2000. Hematopoiesis in larval *Pseudoplusia includens* and *Spodoptera frugiperda*. *Archives of Insect Biochemistry and Physiology* 43: 147-164.

Gupta AP, Campenot ES. 1996. Cytoskeletal F-actin polymerization from cytosolic G-actin occurs in the phagocytosing immunocytes of arthropods (*Limulus polyphemus* and *Gromphadorhina portentosa*): does [cAMP]i play any role? *Journal of Invertebrate Pathology* 68: 118-130.

Krell PJ, Summers MD, Vinson SD. 1982. A virus with a multipartite superhelical DNA genome from the ichneumonid parasitoid *Campoletis sonorensis*. *Journal of Virology* 43: 859-870.

Li X, Webb BA. 1994. Apparent functional role for a cysteine-rich polydnavirus protein in suppression of the insect cellular immune response. *Journal of Virology* 68: 7482-7489.

Luckhart S, Webb BA. 1996. Interaction of a wasp ovarian protein and polydnavirus in host immune suppression. *Developmental and Comparative Immunology* 20: 1-21.

Pech LL, Strand MR. 1996. Granular cells are required for encapsulation of foreign targets by insect haemocytes. *Journal of Cell Science* 109: 2053-2060.

Pennacchio F, Falabella P, Vinson SB. 1998. Regulation of *Heliothis virescens* prothoracic glands by *Cardiochiles nigriceps* polydnavirus. *Archives of Insect Biochemistry and Physiology* 38: 1-10.

Prévost G, Davies DH, Vinson SB. 1990. Evasion of encapsulation by parasitoid correlated with the extent of host hemocyte pathology. *Entomologia Experimentalis et Applicata* 55: 1-10.

Schmidt O, Theopold U, Strand M. 2001. Innate immunity and its evasion and suppression by hymenopteran endoparasitoids. *Bioessays* 23: 344-351.

Shelby KS, Webb BA. 1997. Polydnavirus infection inhibits translation of specific growth- associated host proteins. *Insect Biochemistry and Molecular Biology* 27: 263-270.

Shelby KS, Cui L, Webb BA. 1998. Polydnavirus-mediated inhibition of lysozyme gene expression and the antibacterial response. *Insect Molecular Biology* 7: 265-272.

Shelby KS, Adeyeye OA, Okot-Kotber BM, Webb BA. 2000. Parasitism-linked block of host plasma melanization. *Journal of Invertebrate Pathology* 75: 218-225.

Soldevila AI, Heuston S, Webb BA. 1997. Purification and analysis of a polydnavirus gene product expressed using a poly-histidine baculovirus vector. *Insect Biochemistry and Molecular Biology* 27: 201-211.

Soller M, Lanzrein B. 1996. Polydnavirus and venom of the egg-larval parasitoid *Chelonus inanitus* (Braconidae) induce developmental arrest in the prepupa of its host *Spodoptera littoralis* (Noctuidae). *Journal of Insect Physiology* 42: 471-481.

Stettler P, Trenczek T, Wyler T, Pfister-Wilhelm R, Lanzrein B. 1998. Overview of parasitism associated effects on host haemocytes in larval parasitoids and comparison with effects of the egg-larval parasitoid *Chelonus inanitus* on its host *Spodoptera littoralis*. *Journal of Insect Physiology* 44: 817-831.

Strand MR, McKenzie DI, Grassl V, Dover BA, Aiken JM. 1992. Persistence and expression of *Microplitis demolitor* polydnavirus in *Pseudoplusia includens*. *Journal of General Virology* 73: 1627-1635.

Strand MR. 1994. *Microplitis demolitor* polydnavirus infects and expresses in specific morphotypes of *Pseudoplusia includens* haemocytes. *Journal of General Virology* 75: 3007-3020.

Strand MR, Pech LL. 1995. *Microplitis demolitor* polydnavirus induces apoptosis of a specific haemocyte morphotype in *Pseudoplusia includens*. *Journal of General Virology* 76 (Pt 2): 283-291.

Strand MR, Clark KD. 1999. Plasmatocyte spreading peptide induces spreading of plasmatocytes but represses spreading of granulocytes. *Archives of Insect Biochemistry and Physiology* 42: 213-223.

Theilmann DA, Summers MD. 1986. Molecular analysis of *Campoletis sonorensis* virus DNA in the lepidopteran host

Heliothis virescens. *Journal of General Virology* 67: 1961-1969.

Trudeau D, Witherell RA, Strand MR. 2000. Characterization of two novel *Microplitis demolitor* polydnavirus mRNAs expressed in *Pseudoplusia includens* haemocytes. *Journal of General Virology* 81: 3049-3058.

Turnbull MW, Webb BA. 2002. Perspectives on polydnavirus origins and evolution. *Advances in Virus Research* 58: 203-254.

Volkoff A, Ravallec M, Bossy J, Cerutti P, Rocher J, Cerutti M, Devauchelle G. 1995. The replication of *Hyposoter didymator* polydnavirus: Cytopathology of the calyx cells in the parasitoid. *Biology of the Cell* 83: 1-13.

Wago H, Kitano H. 1985. Effects of venom from *Apantales glomeratus* on the hemocytes and hemolymph of *Pieris rapae crucivora*. *Applied Entomology and Zoology* 20: 103-110.

Warren KS, Shutt DC, McDermott JP, Lin JL, Soll DR, Lin JJ. 1996. Overexpression of microfilament-stabilizing human caldesmon fragment, CaD39, affects cell attachment, spreading, and cytokinesis. *Cell Motility and Cytoskeleton* 34: 215-229.

Webb BA, Luckhart S. 1994. Evidence for an early immunosuppressive role for related *Campoletis sonorensis* venom and ovarian proteins in *Heliothis virescens*. *Archives of Insect Biochemistry and Physiology* 26: 147-163.

Webb BA, Luckhart S. 1996. Factors mediating short- and long-term immune suppression in a parasitized insect. *Journal of Insect Physiology* 42: 33-40.

Zar JH. 1996 *Biostatistical Analysis*, 3rd Ed., Prentice Hall.